

## Efficient M-Band Wavelet Based Inpainting Technique to Detect and Impound the Distorted Digital Images

<sup>1</sup>I.Muthulakshmi and <sup>2</sup>Dr. D. Gnanadurai

<sup>1</sup>Assistant Professor / HOD, CSE Department,  
VV College of Engineering, VV Nagar, Tisaiyanvilai 627 657  
Tuticorin District.

*muthulakshmiphd@gmail.com*

<sup>2</sup>Principal, J.P College of Engineering, Ayikudy,  
Tenkaasi - 627 852, Tirunelveli District

### Abstract

*Image inpainting or completion is a technique to restore a damaged image. In this paper M band complex wavelet transform is used for frequency domain conversion of the image subsequently using the iterative shrinkage technique, inpainting process of the cracked image is carried out successfully. In the proposed approach M-band dual tree wavelet transform which decompose the each input wavelets into set of subbands with each sub band wavelets occupying a portion of the original frequency band and hence produced better frequency analysis for image inpainting process. Each sub bands and its coefficients preferentially will be captured different directions and hence it will be detected cracks in different direction. The proposed technique shows better performance than the conventional wavelet based methods. The performance of the proposed approach is evaluated and analyzed by the various cracked images.*

**Keywords:** In painting, wavelets, DWT, Haar, Daubechies, CWT, 2D Dual tree Complex Wavelet transform

### 1. Introduction

Inpainting, the technique of modifying an image in an undetectable form, is as ancient as art itself. The goals and applications of inpainting is numerous, from the restoration of damaged paintings and photographs to the removal/replacement of selected objects [7]. Image inpainting [1, 5] provides a means to restore damaged region of an image, such that the image looks complete and natural after the inpainting process. Applications of image inpainting range from restoration of photographs, films and paintings, to removal of occlusions, such as text, subtitles, stamps and publicity from images. In addition, inpainting can also be used to produce special effects [8]. Traditionally, skilled artists

have performed image inpainting manually. But given its range of applications, it would be desirable to have image inpainting as a standard feature of popular image tools such as PhotoShop. Bertalmio et al [6] have introduced a technique for digital inpainting of still images that produces very impressive results [8]. Digital techniques are starting to be a widespread way of performing inpainting, ranging from attempts to fully automatic detection and removal of scratches in film [3, 19], all the way to software tools that allow a sophisticated but mostly manual process [4].

Cracks usually have low brightness and therefore it is considered as local intensity minima [2]. Inpainting is a technique, used for altering an image in an undetectable form. The main intention of inpainting is the restoration of damaged paintings and photographs for the purging of selected objects [9]. Inpainting is the process of recreating lost or damaged portions of images and videos [15]. Inpainting is an image interpolation technique [16]. In the mathematical field of numerical analysis, interpolation is a technique of creating new data points within the range of a discrete set of known data points [17].

For the crack detection and analysis, several techniques such as neural network, wavelet transform, grid cell analysis (GCA), genetic algorithm (GA), artificial life (AL), fuzzy set theory, texture classification and more has been employed [10]. Wavelet is a promising method, very useful for the detection of structural damages [13]. The 2D discrete wavelet transformation is applied to the model of digital image data in order to find the locality and length of the crack [18]. In mathematics, a wavelet series is a depiction of a square-integrable (real- or complex-valued) function by a certain orthonormal series created by a wavelet [11]. The wavelet transform itself gives great design flexibility. Basis selection, spatial-frequency tiling, and different wavelet threshold approaches can be optimized to achieve best adaptation

for processing application, data characteristics and feature of interest [12]. In wavelet packet transform, the data is transformed using a far more comprehensive range of space-frequency analysis functions, which is expected to mine more information of interest [20].

The structure of the paper is organized as follows: A brief review of the researches related to image inpainting is discussed in Section 2. The proposed wavelet transform based image inpainting is given in Section 3. The experimental results of the proposed approach are presented in Section 4. Finally, the conclusion is given in Section 5.

## 2. Related Work

Gunamani Jena [21] has presented an inpainting algorithm, which implements the filling of damaged region with impressive results. Many algorithms usually required several minutes on current personal computers for the inpainting of relatively small areas. Such a time is unacceptable for interactive sessions and motivated us to design a simpler and faster algorithm capable of producing similar results in just a few seconds. The results produced by the algorithm are two to three orders of magnitude faster to the existing.

I. A. Ismail *et al.* [22] have proposed an integrated technique for the recognition and purging of cracks on digitized images. Using steepest descent algorithm (SDA), initially the cracks have been identified. Then, the identified cracks have been purged using either a gradient Function (GRF) and processed data or a semi-automatic procedure based on region growing. Lastly, crack filling has been performed using the steepest descent method. The proposed technique has been implemented using Matlab, Surfer and Visual Fortran programming. Experimental results have shown that their technique has performed effectively on digitized images suffering from cracks.

Dayal R. Parhi and Sasanka Choudhury [23] have conducted a comprehensive review of several techniques in the field of crack detection in Beam-Like Structure. Sensibility analysis of experimentally measured frequencies as a decisive factor for crack identification has been employed widely in the last few decades because of its straightforwardness. But, the determination of crack parameters such as depth and location is complicated. Several techniques have been discussed on the basis of dynamic analysis of Crack. The techniques mostly used for crack detection were fuzzy logic neural network, fuzzy system, hybrid neuro genetic algorithm, artificial neural network, artificial intelligence.

K.N.Sivabala and D.Gananadurai [24] have utilized Gabor filter and Gaussian filter in order to remove the texture elements in the digital image by separating the

defected area. Then, a fast searching algorithm which uses feature extraction parameters has been proposed to find the defected pixels and to robustly segment it. Their proposed method was appropriate for both texture and non texture images. Consequently, the algorithm has successfully detected the damage in the digital texture image using non texture methods.

J. Rupil *et al.* [25] have introduced a digital image correlation technique for recognizing and calculating automatically the micro cracks on the surface of a specimen during a fatigue test. The technique has allowed a quick scanning of the entire surface with all possible (pixel-wise) locations of micro crack centers and the detection of cracks containing a sub-pixel opening. An experimental test case has been presented as a design of the method and a comparison has been conducted with a replica technique

YANG Jian-bin *et al* [14] used dual-tree complex wavelet transform tool in signal and image processing. This paper proposed a dual-tree complex wavelet transform (CWT) based algorithm for image inpainting problem. The approach is based on Cai, Chan, Shen and Shen's framelet-based algorithm. The complex wavelet transform outperforms the standard real wavelet transform in the sense of shift-invariance, directionality and anti-aliasing. Numerical results illustrate the good performance of algorithm.

## 3. Wavelets Based Image Inpainting

Let 'a' be an image in the domain 'D'

$$a = \{ a_{ij} ; 1 < i \leq P, 1 < j \leq Q \} \quad (1)$$

And the  $a'$  be known, observed region and  $\hat{D}$  is the inpainting domain. The intensity value

$$v(a_i) = v_0(i) + \Delta(i) \quad (2)$$

in the domain 'D' where  $\Delta$  is the noise term. The proposed system finds an image 'b' that matches  $V_0$  in 'D' and have meaningful content in the domain  $\hat{D}$  since the value of  $v(a_i)$  is arbitrary when  $i \in \hat{D}$ . The proposed system consists of the following steps (a) Initial value assignment, (b) Converting to frequency domain (c) coefficients thresholding, (d) Reconstruction, (e) Iterative image inpainting.

### 3.1. Initial Value Assignment Using Nearest Neighbor Algorithm

Initially the closest entries of  $a'$  are identified and replaced using nearest neighbor algorithm. The selection of closest entries can be realized in two methods, first, as is, on the set of entities, and, second by considering only entities with non missing entries in

the attribute corresponding to that of target's missing entry. The proposed system uses the second approach for initial assignment of the damaged portion. The following procedure represents the nearest neighbor algorithm.

**Procedure 1: Nearest Neighbor Algorithm**

- Step 1: Read an initial value  $a_i'$
- Step 2: Find K neighbors of  $a_i'$
- Step 3: Find the data matrix  $a_i''$  consisting of  $a_i'$  and K neighbors
- Step 4: Apply an imputation algorithm to  $a_i''$  and impute missing values in  $a_i'$
- Step 5: Repeat the above steps until  $a_i'$  are filled.

**3.2. Conversion of Image to Frequency Domain By Means of Wavelet**

The proposed system uses the M-band Complex 2 D Dual tree wavelet transform

which possesses the unique geometrical features for frequency domain conversion. This decomposition provides local, multi-scale directional analysis. The wavelet transform is self possessed of cascading M-band filter banks. The Mband trees are obtained by performing two M-band multi resolution analyses in parallel in the real case, or four in the complex case. The dual tree decompositions are shift variant, with each trend keeping the same characteristics when the data is delayed. Different sub bands and two sets of coefficients preferentially capture different directions.

The M-band bi-orthogonal wavelet decomposition of  $L^2(R)$  is based on the joint use of two sets of basic functions  $\psi_0 \leq m < M, \bar{\psi}_m \leq m < M$  which satisfy the following scaling equations expressed in the frequency domain.

$$M^{1/2} \psi_m(M\omega) = H_0(\omega) \psi_0(\omega) \tag{3}$$

$$M^{1/2} \hat{\psi}_m(M\omega) = H_0(\omega) \hat{\psi}_0(\omega) \tag{4}$$

Here  $\psi_0$  is the father wavelet and  $\bar{\psi}_m$  are mother wavelets.  $m \in \{1, \dots, M-1\}$  which defined a dual M-band multi resolution analysis. Specifically the mother wavelets will be obtained by Hilbert transform. In the Fourier domain the desired property reads,

$$|\hat{\psi}_m(\omega)| = -i \operatorname{sign}(\omega) \hat{\psi}(\omega), \quad \{\forall m \in \{1, \dots, M-1\}\}$$

The sign is the signum function and  $\hat{d}$  designates the Fourier transform of a function d. The Hilbert condition (4) yields

$$\{\forall m \in \{1, \dots, M-1\}\} |\hat{\psi}_m^H(\omega)| = |\hat{\psi}_m(\omega)| \tag{5}$$

The scaling equation leads to

$$\{\forall m \in \{1, \dots, M-1\}\} G_m(\omega) = e^{-i\theta_m(\omega)} H_m(\omega) \tag{6}$$

Where  $\theta_m$  is  $2\pi$  periodic. The frequency phase functions should also be odd (for real filters) and thus only need to be determined over  $[0, \pi]$ . In the 2 band case (under weak assumptions)  $\theta_m$  is a linear function on  $[-\pi, \pi]$ . In the M band the constraint is slightly restricted on a smaller interval by imposing

$\{\forall \omega \in [0, 2\pi/M], \theta_0(\omega) = \zeta \omega$  where  $\zeta \in R$ . It can be deduced that, Para-unitary M band filter bank conditions are obtained by choosing the phase functions defined by

$$\{\forall p \in \{0, \dots, \lfloor \frac{M}{2} \rfloor - 1\}, \forall \omega \in [\frac{pM+2\pi}{M}, (p+1)\frac{2\pi}{M}], \theta_0 = (d + \frac{1}{2})(M-1)\omega - p\pi, \tag{7}$$

$$\{\forall m \in \{1, \dots, M-1\}, \theta_m(\omega) \in \begin{cases} \frac{\pi}{2} - (d + \frac{1}{2})\omega & \text{if } \omega \in [0, 2\pi], \\ 0 & \text{if } \omega = 0 \end{cases} \tag{8}$$

Where

Where  $d \in Z$  denotes the upper integer part of real u. The scaling function associated to the dual wavelet composition is such that

$$\{\forall k \in N, \forall \omega \in [2k\pi, 2(k+1)\pi], \hat{\psi}_0^H(\omega) = (-1)^k e^{-i(d+\frac{1}{2})\omega} \hat{\psi}_0(\omega) \tag{9}$$

Find that except in the 2 band case  $\theta_0$  exhibits discontinuities on  $0, \pi$  due to the  $p\pi$  term.

The two dimensional separable M-band wavelets bases can be derived from the 1 D dual tree decomposition. Thus we obtain two bases of  $L^2(R^2)$ . The first one corresponds to the classical 2d separable wavelet basis but the second one results from the tensor product of the dual wavelet basis function. A discrete implementation of these wavelet decompositions starts from level  $j=1$  to go up to the coarsest resolution level  $j \in N^*$ . The decomposition on to the former 2D wavelet

basis function yields coefficients  $\delta_{j,m,m}^H[k,l]$ , whereas the decomposition on to the dual basis generates coefficients

$$\delta_{j,m,m}^H[k,l]$$

The wavelet transform is a continuous-space formalism which is applied to the discrete image. The analog scene corresponds to the 2D field

$$f(p, q) = \sum_{g, l} f(g, l) x(p - g, q - l), \quad (10)$$

Here the 'x' is the interpolation functions and  $f(g, l)_{(g, l) \in \mathbb{Z}^2}$  is the image sample sequence. The image is project on to the approximation space

$$V_0 = \text{span} \{ \psi_0(p - g) \psi_0(q - l) | (k, l) \in \mathbb{Z}^2 \}. \quad (11)$$

The projection of 'f' reads

$$EV_0(f(p, q)) = \sum_{k, l} \delta_{0,0,0}[k, l] \psi(p - q) \psi(q - l) \quad (12)$$

Where the approximation coefficients are

$$\delta_{0,0,0}[g, l] = f(y, z) \lambda_x, \Psi_{0,0}(k - y, l - z) \quad (13)$$

Where  $\Psi_{0,0}([p, q]) = \psi_0(p) \psi_0(q)$  and  $\lambda_x, \Psi_{0,0}$  (14)

Is the cross-correlation function defined as

$$\lambda_x, \Psi_{0,0} = \int_{-\infty}^{\infty} \int_{-\infty}^{\infty} x(u, v) \psi_{0,0}(u - p)(v - q) dudv \quad (15)$$

Similarly the analog image is projected on to the dual approximation space

$$V_o^H = \text{span} \{ \psi_{0,0}^H(p - g, q - l), (k, l) \in \mathbb{Z}^2 \} \quad (16)$$

$$\text{Where } \Psi_{0,0}^H([p, q]) = \psi_0^H(p) \psi_0^H(q) \quad (17)$$

Then the dual approximation coefficients are given by

$$\delta_{0,0,0}^H[g, l] = f(y, z) \lambda_x, \Psi_{0,0}(k - y, l - z) \quad (18)$$

Obviously Eq.(13) and (18) can be interpreted as the use of two of pre filters on the discrete image

$f(g, l)_{(g, l) \in \mathbb{Z}^2}$  before the dual tree decomposition and the frequency responses of these filters are

$$H1(\omega_x, \omega_y) = \sum_{u=-\infty}^{\infty} \sum_{v=-\infty}^{\infty} \hat{s}(w_x + 2y\pi, \omega_q + 2z\pi) \psi_0^*(\omega_q + 2Z\pi) \quad (19)$$

$$H2(\omega_p, \omega_q) = e^{i(d+1/2)\omega_p, \omega_q} H1(\omega_p, \omega_q) \quad (20)$$

Different kinds of interpolation function may be considered, for instance the separable functions of the form  $x(p, q) = \phi(p)\phi(q)$ . the two pre filters are then separable with the impulse responses  $\lambda\phi, \psi_0(p)$ ,  $\lambda\phi, \psi_0(q)$  and  $\lambda\phi, \psi_0^H(y)$ ,  $\lambda\phi, \psi_0^H(z)$  respectively.

### 3.2.1. Direction Extraction in the Different Sub Bands

Some linear combinations of the primal and dual sub bands are used to extract the local directions present in the image. The defined analytic wavelets for direction sub bands are

$$\psi_m^k(t) \frac{\psi_m(t)}{2^{1/2}} + i \psi_m^H(t) \quad (21)$$

$$\psi_m^k(t) \frac{\psi_m(t)}{2^{1/2}} - i \psi_m^H(t) \quad (22)$$

The tensor product of the two analytic wavelets

$$\psi_m^k \text{ and } \psi_m^H$$

And the real part of the tensor product is

$$\psi_{m,m}^a(x, y) = \text{Re} \{ \psi_m^k(p) \psi_m^H(q) \} \quad (23)$$

For  $m, m' \in \{1, \dots, M - 1\}^2$  the Fourier transform of this function is equal to

$$\hat{\psi}_{m,m}^a(\omega_p, \omega_q) = \begin{cases} \psi_p(\omega_p) \psi_m(\omega_q) & \text{if } \text{sign}(\omega_x) = \text{sign}(\omega_y), \\ 0 & \text{if } \text{sign}(\omega_x) \neq \text{sign}(\omega_y), \end{cases} \quad (24)$$

The above function allows us to extract the directions that falling in the first third quadrant of the frequency plane. Like wise the real part of the tensor product of an analytic wavelet and anti analytic one is

denoted by  $\psi_{m,m}^a$ . This function is used to select the frequency components which are localized in the second /fourth quadrant of the frequency plane. This corresponds to opposite directions to those obtained

with  $\hat{\psi}_{m,m}^a$

At a given resolution level r, for each sub band  $m, m'$  with  $m \neq 0$  and  $m' \neq 0$ , the directional analysis is achieved by computing the coefficients

$$C_{r,m,m'}[k, l] = (f(p, q), \frac{1}{M^r} \psi_{m,m}^a(\frac{x}{M^r} - k, \frac{y}{M^r} - l)) \quad (25)$$

$$C_{r,m,m'}[k, l] = (f(p, q), \frac{1}{M^r} \psi_{m,m}^a(\frac{x}{M^r} - k, \frac{y}{M^r} - l)) \quad (26)$$

According to equation (21), (22) and (23) for all  $m, m' \in \{1, \dots, M - 1\}^2$

$$C_{r,m,m'}[k, l] = \frac{1}{\sqrt{2}} \delta_{r,m,m'}[k, l] + \delta_{r,m,m'}^H[k, l] \quad (27)$$

$$C_{r,m,m'}^H[k, l] = \frac{1}{\sqrt{2}} \delta_{r,m,m'}[k, l] - \delta_{r,m,m'}^H[k, l] \quad (28)$$

### 3.2.2. Coefficients Thresholding

Initially the diagonal matrix  $\Delta D$  is obtained as follows.

$$\Delta D_{ij} = \begin{cases} 1 & \text{if } a_{ij} \in \eta \\ 0 & \text{if } a_{ij} \notin \eta \end{cases} \quad (29)$$

Subsequently the initial guess of the original image is done. by using the For  $n=1, 2, \dots$

$f_n = \Psi^* Shrink(\Psi_l, \lambda)$ . By using the shrinkage procedures as in [14] are carried out for all the M-bands of 2DCWT coefficients. As follows

$$shrink(u, \lambda) = \begin{cases} 0 & \text{if } |u| \leq \lambda \\ \frac{|u| - \lambda}{|u|} \cdot u & \text{if } |u| > \lambda \end{cases} \quad (30)$$

Where 'l' is the given intensity. And then the iterative algorithm

$$l_{n+1} = \Delta D l + (I - \Delta D) f_l \quad (31)$$

is repeated until the 'n' convergence. Using [25], if  $\mathcal{E}(i) = 0$  for every values  $l^*$  is the output of (35) then  $\Gamma$  of  $\eta$  (1), then it will be the solution of the interpolation problem. Otherwise the solution  $l^* = \Psi^* Shrink(\Psi_l^*, \lambda)$  will be the denoising and interpolation problem.

### 3.2.3 Reconstruction

Let  $f$  be the vector of image samples,  $\delta$  the vector of coefficients produced by the primal M band decomposition and  $\delta^H$  be the vector of coefficients produced by dual one. The global decomposition operator is

$$D : f \rightarrow \begin{pmatrix} C \\ C^H \end{pmatrix} = \begin{pmatrix} D_1 f \\ D_2 f \end{pmatrix} \quad (32)$$

Where  $D_1 = U_1 F_1$  and  $D_2 = U_2 F_2$   $F_1$  and  $F_2$  being the pre filtering operations and  $U_1$  and  $U_2$  be the orthogonal m band decomposition then the following can be proved. Assume that  $x(p-g, q-l)_{g,l \in \mathbb{Z}^2}$  is an orthonormal family of  $L^2(\mathbb{R}^2)$ . Provided that there exist  $I_e J_e I_{\nu_0} \in (R_+^*)^3$  for almost all  $\omega_x, \omega_y \in [-\pi, \pi]^2$ ,

$$|\hat{x}(\omega_x, \omega_y)| < I_e, |\hat{\psi}(\omega_x)| \geq A \psi_0 \quad (33)$$

$$\sum_{(p,q) \neq (0,0)} |x(\omega_p + 2y\pi, \omega_q + 2z\pi)|^2 \leq J_x < I_x^2 I_{\nu_0}^4 \quad (34)$$

The D is the frame operator. The "dual" frame reconstruction operator is given by

$$I = (F_1^* F_1 + F_2^* F_2)^{-1} (F_1^* U_1^{-1} \delta + F_2^* U_2^{-1} \delta^H) \quad (35)$$

Where  $F_1^*$  designates the adjoint of an operator  $F_1$ . The formula (32) minimizes the impact of possible errors in the computation of the wavelet coefficients.  $U_1^{-1}$  and  $U_2^{-1}$  are the inverse of M-

band wavelet transforms and  $F_1^*, F_2^*$  and  $((F_1^* F_1 + F_2^* F_2)^{-1})$  correspond to filtering with frequency responses.  $|F_1^*(\omega_p, \omega_q)|^2, |F_2^*(\omega_p, \omega_q)|^2$  and  $(|F_1(\omega_p, \omega_q)|^2 + |F_2(\omega_p, \omega_q)|^2)^{-1}$  respectively.

## 4. Experimental Results

The proposed image inpainting system is implemented in MATLAB platform (version 7.10) and it is evaluated using the various images. Also the performance of the proposed wavelet based inpainting system is tested and analyzed by increasing the crack level. The (a),(b),(c) of Figure 1, Figure 3, Figure 5, Figure 7 and Figure 9 represents the three levels of cracked images and (d),(e),(f) of those images represents the inpainted images using the proposed technique. The performance of the proposed technique is analyzed quantitatively by using the metrics Peak Signal to Noise Ratio (PSNR) and standard deviation to mean ratio (S/M).

The performance of the proposed technique is also evaluated by comparing it with the inpainting techniques using the wavelets DWT, Haar, Daubechies, and CWT based technique. The table 1, 2 and 3 represents the psnr values of the inpainted images and evaluation values. The Figure. 11 and Figure. 12 represents the PSNR mean ratio comparison graph of the proposed technique with the other inpainting techniques using the comparison wavelets. Like wise the Figure. 13 represents the S/M comparison graph.



**Figure 1:** The cracked and inpainted image-1 (Proposed Approach)

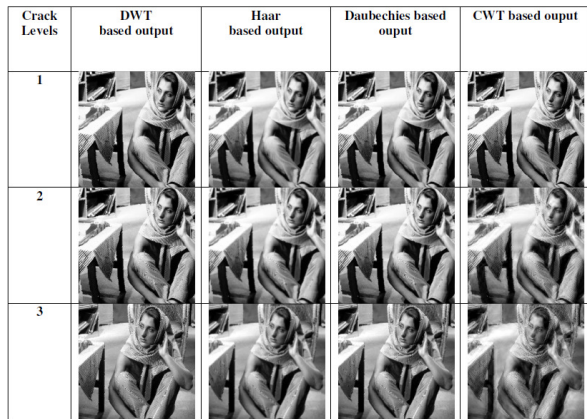


**Figure 2:** In painted output images using various comparison wavelets for image-1.

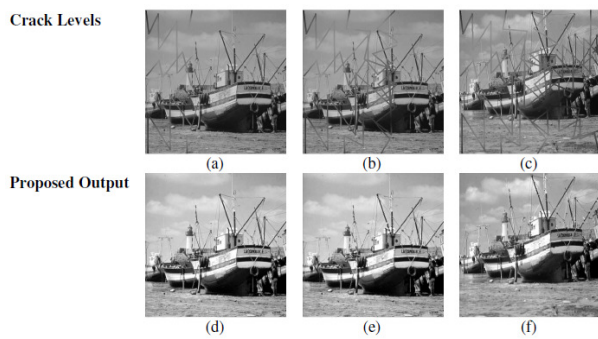


**Figure 3:** The cracked and inpainted image-2(Proposed Approach)

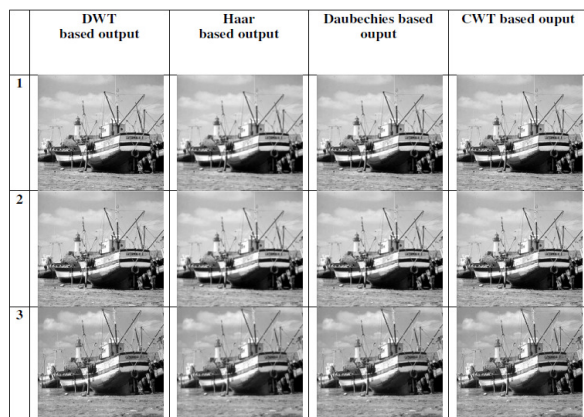


**Figure 4:** In painted output images using various comparison wavelets for image-2.

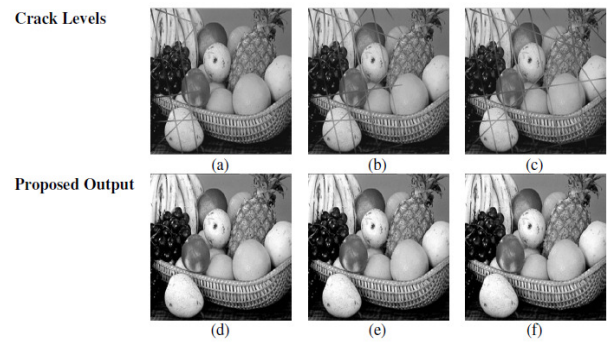


**Figure 5:** The cracked and inpainted image-3(Proposed Approach)

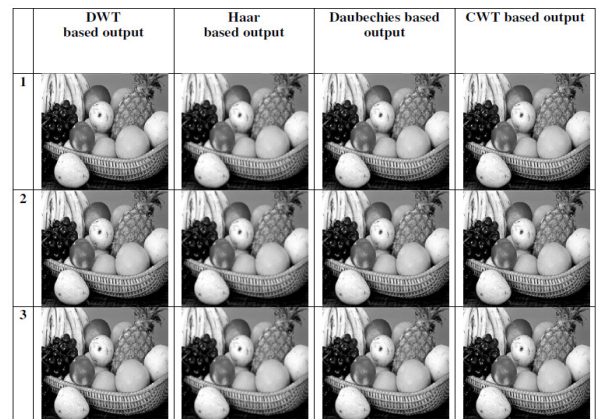


**Figure 6:** In painted output images using various comparison wavelets for image-3.

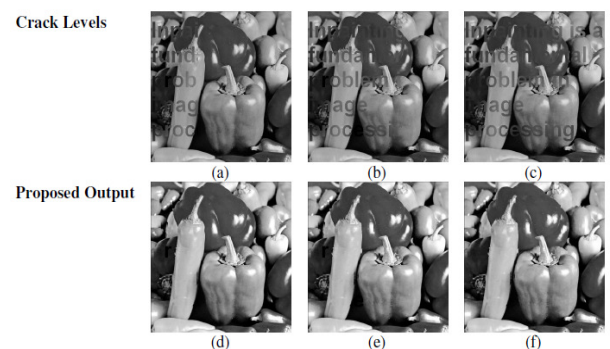


**Figure 7:** The cracked and inpainted image-4(Proposed Approach)

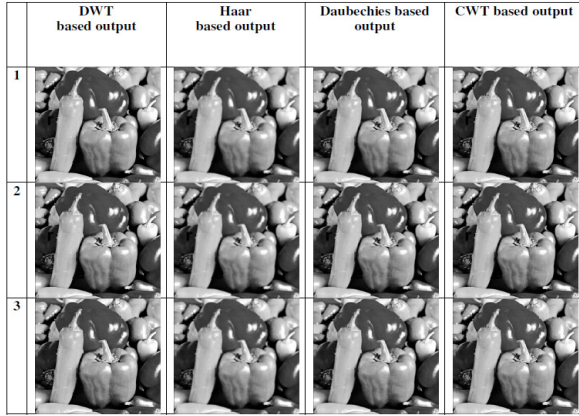


**Figure 8:** In painted output images using various comparison wavelets for image-4.



**Figure 9:** The cracked and inpainted image-5(Proposed Approach)

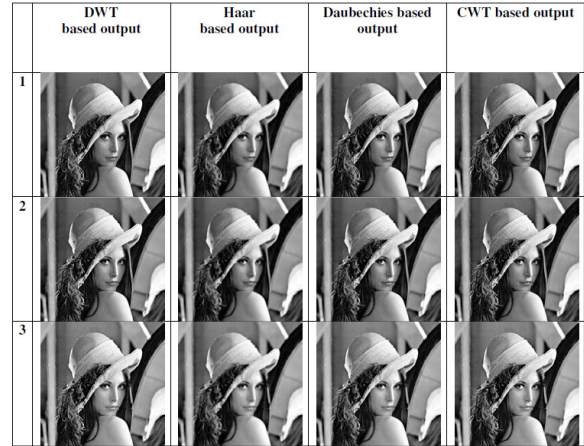


**Figure 10:** In painted output images using various comparison wavelets for image-5.

**Table 1:** Performance comparison table\_1(PSNR)

	Image1	Image2	Image3	Image4	Image5	Total	Average	Standard deviation	S/M
<b>DWT</b>	15.682659	17.38496	17.204759	16.78396	19.2851	86.34143	17.26829	1.307092	0.075693
<b>Haar</b>	14.702661	16.87209	17.003936	16.52693	18.72821	83.83382	16.76676	1.43463	0.085564
<b>Daubechies</b>	14.74743	17.06256	17.133125	16.59035	18.96635	84.49982	16.89996	1.506654	0.089151
<b>CWT</b>	15.528204	17.34496	17.211023	16.71531	19.22632	86.02581	17.20516	1.337609	0.077745
<b>Proposed</b>	15.668087	17.3652	17.218906	16.77732	19.23909	86.26859	17.25372	1.29388	0.074991

**Table 2:** Performance comparison table\_2(PSNR)

	Image1	Image2	Image3	Image4	Image5	Total	Average	Standard deviation	S/M
DWT	12.31413	13.62292	15.3487	14.82145	15.72731	71.83451	14.3669	1.395405	0.097126
Haar	11.84051	13.33268	15.2288	14.66204	15.5623	70.62632	14.12526	1.534543	0.108638
Daubechies	11.86531	13.46868	15.29738	14.73502	15.62703	70.99343	14.19869	1.542118	0.10861
CWT	12.18224	13.58814	15.35559	14.80449	15.70939	71.63985	14.32797	1.444204	0.100796
Proposed	12.29484	13.61145	15.37255	14.82146	15.75517	71.85546	14.37109	1.415034	0.098464

**Table 3:** Performance comparison table\_3(PSNR)

	Image1	Image2	Image3	Image4	Image5	Total	Average	Standard deviation	S/M
DWT	11.38259	13.32602	14.08648	13.54998	12.84451	65.18958	13.03792	1.027402	0.078801
Haar	11.18111	13.05052	13.99956	13.38804	12.70727	64.32649	12.8653	1.055409	0.082035
Daubechies	11.16304	13.16882	14.04156	13.44157	12.81528	64.63029	12.92606	1.082766	0.083766
CWT	11.33501	13.28759	14.09376	13.48232	12.84611	65.04478	13.00896	1.037682	0.079767
Proposed	11.45881	13.30298	14.11342	13.52093	12.89258	65.28872	13.05774	0.99662	0.076324

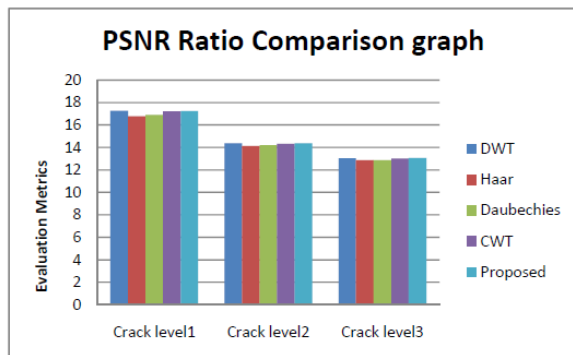


**Figure 11:** Performance Comparison graph\_1

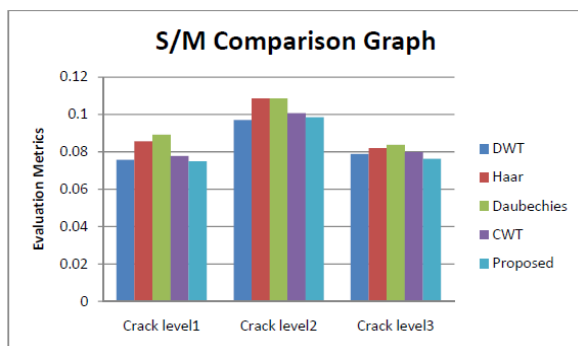


**Figure 12:** Performance Comparison Graph\_2

From the table-1, it is clear that, the proposed approach has achieved (-0.01457,0.486954,0.353755,0.048556 PSNR values than the DWT, Haar, Daubechies and CWT based inpainting techniques for crack level1. Like wise from table 2 and table3 illustrates that the proposed approach achieved (0.00419, 0.245828, 0.172406 and 0.043122) and (0.019828, 0.192445, 0.131687 and 0.048789) for crack level-2 and crack level3 respectively. Also the Figure11 and Figure12 represents the higher performance of the proposed inpainting technique. Though the psnr value of proposed approach is little deviated than the dwt based approach for crack level1,

The standard deviation values and S/M values shows the better result of the proposed approach.

### 5. Conclusion

In this paper, 2D CWT\_M band based iterative image inpainting approach was proposed. The approach was implemented and experimented with different images with various crack level also the proposed approach was compared with the various inpainting techniques with different wavelets. The analytical results confirmed that the proposed approach has shown a better performance than the other comparative wavelets based approaches. Overall, the proposed approach has achieved 0.032192%, 2.00223%, 1.419495%, 0.318375% more PSNR values than the traditional DWT, Haar, Daubechies and CWT based inpainting techniques (i.e) In the circumstance of achieving 100% performance by proposed approach, the other comparative wavelets based inpainting approaches are able to achieve only 99.97%, 98%, 98.59% 99.68% for DWT, Haar, Daubechies and CWT) respectively. Such performance has been achieved because of the M band nature of 2d dual tree complex wavelet transform and its improved directional analysis as well as frequential analysis feature.

### References

- [1] Chen, Fang; Suter, David; "Motion Estimation for Noise Reduction in Historical Films: MPEG Encoding Effects,"In Proceedings of 6th Digital Image Computing: Techniques and Applications (DICTA2002) Conference, pp. 207-212, 2002.
- [2] Sachin V. Solanki and A. R. Mahajan,"Cracks Inspection and Interpolation in Digitized Artistic Picture using Image Processing Approach",International Journal of Recent Trends in Engineering, Vol. 1, no. 2, May 2009.
- [3] A.C. Kokaram, R.D. Morris, W.J. Fitzgerald, P.J.W. Rayner, "Detection of missing data in image sequences", IEEE Transactions on Image Processing 11(4), 1496-1508, 1995.
- [4] C. Braverman, "Photoshop retouching handbook "IDG Books Worldwide, 1998.
- [5] Joyeux, L.; Buisson, O.; Besserer, B.; Boukir, S.; "Detection and Removal of Line Scratches in Motion Picture



- Films," IEEE Computer Society Conference on Computer Vision and Pattern Recognition, pp. 548—553,1999.
- [6] Bertalmio, M, Sapiro, G., Caselles, V., Ballester, C. Image Inpainting. , pp 417-424, SIGGRAPH 2000.
- [7] By Marcelo Bertalmio , Guillermo Sapiro,"Image Inpainting", 2000.
- [8] Manuel M. Oliveira, Brian Bowen Richard, McKenna Yu-Sung Chang, "Fast Digital Image Inpainting", Appeared in the Proceedings of the International Conference on Visualization, Imaging and Image Processing (VIIP 2001), Marbella, Spain.September 3-5, 2001.
- [9] Marcelo Bertalmio, Guillermo Sapiro, Vicent Caselles and Coloma Ballester, "Image inpainting", Proceedings of the 27th annual conference on Computer graphics and interactive techniques, 2000.
- [10]Yong Hu and Chun-xia Zhao,"A Local Binary Pattern Based Methods for Pavement Crack Detection",Journals of pattern recognition research,2009.
- [11]."Wavelet transform",[http://en.wikipedia.org/wiki/Wavelet transform](http://en.wikipedia.org/wiki/Wavelet_transform)
- [12]"Wavelets in Medical Image Processing: De-noising, Segmentation, and Registration",[www.loni.ucla.edu/twiki/pub/CCB/CcbBiologicalProjects/91-pdf.pdf](http://www.loni.ucla.edu/twiki/pub/CCB/CcbBiologicalProjects/91-pdf.pdf)
- [13]Mohammad Ali Lotfollahi-Yaghin and Mohammad Amin Hesari,"Using Wavelet Analysis in Crack Detection at the Arch Concrete Dam under Frequency Analysis with FEM",World Applied Sciences Journal,vol.3,no.4,pp.691-704,2008.
- [14] YANG Jian-bin, "Image inpainting using complex 2-D dual-tree wavelet transform",Applied Mathematics,Vol. 26, No.1, pp.70-76,Applied Mathematics - A Journal of Chinese Universities,2011.
- [15]"Inpainting",<http://en.wikipedia.org/wiki/Inpainting>
- [16]"Application of variational partial differential equation models in medical image processing ", [http://etd.fcla.edu/UF/UFE0004327/huang\\_f.pdf](http://etd.fcla.edu/UF/UFE0004327/huang_f.pdf)
- [17]"Interpolation",<http://en.wikipedia.org/wiki/Interpolation>
- [18] I. A. Ismail, E. A. Rakh, S. I. Zaki, M. A. Ashabrawy, M. K. Shaat,"Perceptible Grouping of Cracks in nuclear piping using wavelet transformation",International Journal of Computer and Electrical Engineering, Vol. 1, No. 5 December, 2009
- [19] A.C. Kokaram, R.D. Morris, W.J. Fitzgerald, P.J.W. Rayner, "Interpolation of missing data in image sequences", IEEE Transactions on Image Processing Vol.11, No.4, pp. 1509-1519, 1995.
- [20] M. Browne, M. Dorn, R. Ouellette, T. Christaller and S. Shiry, "Wavelet Entropy-based Feature Extraction for Crack Detection in Sewer Pipes", proceeding of the 6th International Conference on Mechatronics Technology, 2002.
- [21]Gunamani Jena,"Restoration of Still Images using Inpainting techniques", International Journal of Computer Science & Communication,Vol. 1, no. 2, , pp. 71-74, July-December 2010.
- [22]I. A. Ismail, E. A. Rakh, S. I. Zaki, M. A. Ashabrawy, M. K. Shaat,"Crack detection and filling, using steepest descent method",International Journal of Computer and Electrical Engineering, Vol. 1, no. 4, October, 2009.
- [23] Dayal R. Parhi and Sasanka Choudhury,"Analysis of smart crack detection methodologies in various structures", Journal of Engineering and Technology Research Vol. 3,no.5, pp. 139-147, May 2011.
- [24]K.N.Sivabala and D.Gananadurai,"Efficient defect detection algorithm for gray level digital images using gabor wavelet filter and gaussian filter" International Journal of Engineering Science and Technology (IJEST),Vol. 3 no. 4 ,Apr 2011
- [25] J. Rupil, S. Roux,F. Hild,and L.Vincent,"Fatigue micro crack detection with digital image correlation", The Journal of Strain Analysis for Engineering Design,vol. 46,no. 6 ,2011.